Chapter 2 *Experimental Methods*

2.1 Introduction

Nanostructured transition metal oxides (TMOs) including powders and thin films, are synthesized using various conventional methods such as hydrothermal route, sol-gel technique, precipitation, co-precipitation, high energy ball milling, polymer pyrolysis, spin coating, electron beam evaporation, RF sputtering, ion beam sputtering, molecular beam epitaxy etc. An environment friendly green synthesis method is also used in recent years to prepare powder samples. Each synthesis method has its own technical advantages and disadvantages since the stoichiometry, crystalline phase, size and shape can be altered by varying the synthesis methods which gives rise to significant variation in their properties. Therefore, the selection of synthesis method is an important step to have desired structure, microstructure and properties. In this chapter, a facile and cost-effective sol-gel technique along with the environment friendly green synthesis method is adopted to synthesize pure and rare earth doped HfO_2 nanoparticles which is given in section 2.2. In section 2.3, we have discussed the ion beam sputtering and molecular beam epitaxy methods for deposition of HfO_2 thin films. The fabrication methods of memory devices based on HfO_2 thin films are presented in section 2.4. A concise working principle and operational details of different characterization techniques used for investigating the HfO_2 nanostructures are described in section 2.5.

2.2 Synthesis of Nanoparticles

We used conventional sol-gel technique and environment friendly green synthesis method to synthesize HfO_2 nanoparticles.

2.2.1 Sol-gel Technique

The flow chart of the synthesis of HfO_2 nanoparticles via a simple Pechini type sol-gel technique is given in **Figure 2.1**. For pure HfO_2 nanopowders, the stoichiometric amount of hafnium chloride ($HfCl_4$, 99.9%, Alfa Aesar) was mixed with 2M citric acid ($C_6H_8O_7$) solution under constant stirring using a Teflon coated magnetic bead. Pr doped HfO_2 nanoparticles with varying concentration were synthesized by addition of appropriate amount of praseodymium nitrate ($Pr(NO_3)_3$, 99.9%, Alfa Aesar) to the aforementioned solution mixture.

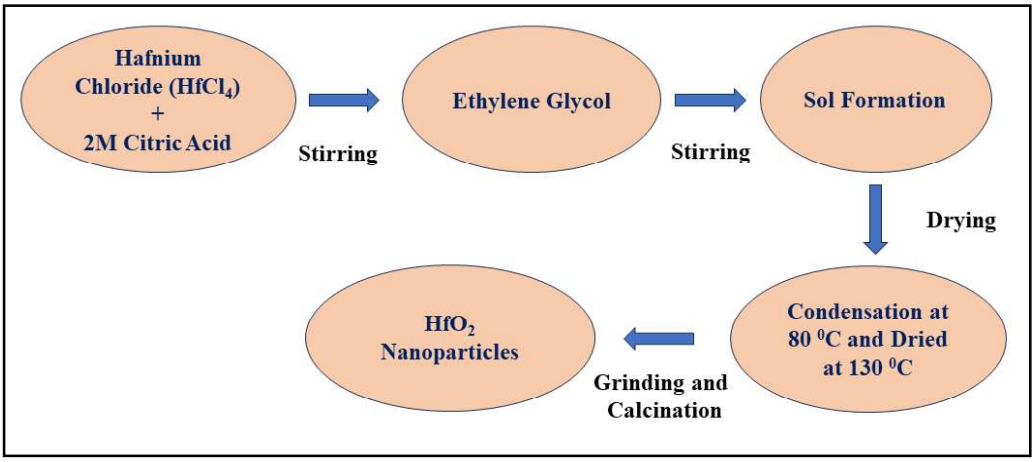

Figure 2.1 *Flow chart of sol-gel technique for the synthesis of pure HfO_2 and Pr doped HfO_2 nanopowders.*

Afterwards, we got a transparent solution ensuring complete dissolution of different precursors. After adding ethylene glycol (EG) ($C_2H_6O_2$) into the prepared solution the sol polymerized and became transparent. After heating the sol at 80 °C for 5 h to complete the condensation process, the sol was dried at 120 °C for 20 h in order to get the precursor resin. Thereafter, the dried-out product was crushed into fine powder using an agate mortar and pestle. The prepared fine powder was slightly brown in color owing to the presence of organic impurities. Finally, the synthesized powders were calcined at 900 °C in a muffle furnace for 5 h to get white colored pure HfO_2 and Pr doped HfO_2 nanoparticles.

2.2.2 Green Synthesis Method

We used orange peel extracts as biomaterials for the green synthesis of HfO_2 nanoparticles. Briefly, oranges were initially washed with deionized water, followed by subsequent wiping. The peeled-off orange skins (peels) were then dried in an oven at 65 °C for 9 h. Dried peels were further ground into moderately fine powder with a mortar and pestle. The required amount of orange peel powder (1, 2 and 4 g) was taken in a beaker with 100 ml of deionized water. The solution mixture was stirred for 3 h at room temperature. Then the mixture was kept in a water bath at 60 °C for 60 min. After cooling down to room temperature, the mixture was filtered first with a muslin cloth and then with a Whatman grade 2 filter paper. The filtered orange peel extract was kept in an airtight Nalgene bottle at 4 °C for further use. HfO_2 nanoparticles were synthesized using a green sol-gel method. Briefly, 3 g of hafnium chloride ($HfCl_4$, 99.9%, Fisher Scientific) was mixed with 45 ml of 1 wt% orange peel extract. The solution was stirred for 60 min at room temperature and then placed in a water bath at 60 °C for 60 min. Afterwards, the solution was dried at 100 °C for 2 h and ground into fine powder. The sample was then

calcined at 900 °C for 1 h using a porcelain crucible with lid in a muffle furnace. **Figure 2.2** shows a schematic of the green synthesis of HfO_2 samples using orange peel extracts.

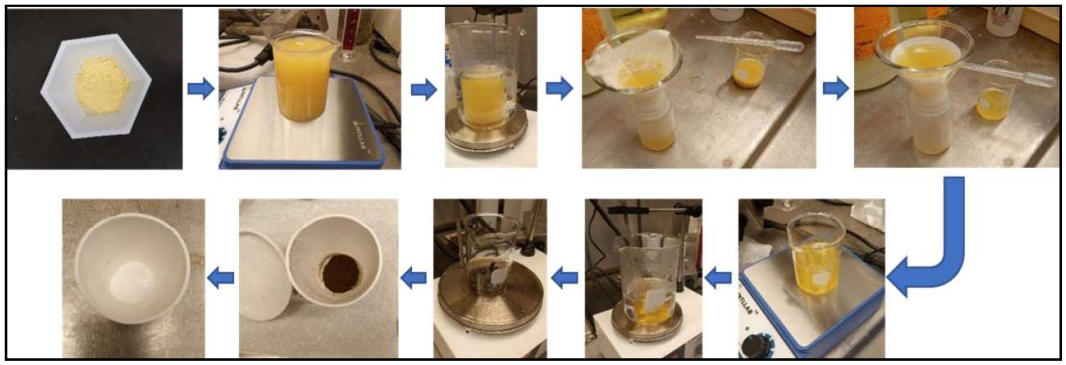

Figure 2.2 *Schematic diagram of HfO_2 synthesis from orange peel extracts via green sol-gel route.*

Following the above method, HfO_2 nanoparticles were also synthesized using 2 and 4 wt% of orange peel extract. The HfO_2 nanoparticle synthesized using 1 wt% orange peel extract (OPE) was denoted as HO-1-OPE. Similarly, the HfO_2 nanoparticles synthesized using 2 and 4 wt% OPE were denoted as HO-2-OPE and HO-4-OPE, respectively.

2.3 Deposition of Thin Films

To fabricate HfO_2 thin films, we utilized the ion beam sputtering and molecular beam epitaxy techniques.

2.3.1 Ion Beam Sputtering (IBS)

Ion beam sputtering (IBS) is a physical vapor deposition (PVD) technique that offers superior precision and control compared to other thin film deposition methods such as thermal evaporation, DC/RF magnetron sputtering, and pulsed laser deposition (PLD). IBS achieves high quality due to its use of low chamber pressure and high-energy ions

striking the target material. This method provides numerous advantages, including uniform layer deposition, stability, precise thickness control, and versatility in material choice (metals, insulators/dielectrics, magnetic materials, and refractory metals). During the IBS process, a broad beam of collimated ions hits the target, causing target atoms or molecules to be sputtered and subsequently deposited on the substrate. Typically, inert gas ions (such as Argon or Xenon) are used; when these ions strike the target, they dislodge atoms or molecules, which then possess high kinetic energy (1-10 eV), resulting in the formation of a compact, pinhole-free thin layer.

An IBS deposition chamber contains several essential components, including the ion source, target and substrate holder. In the ion source, a high voltage ranging from 2 to 10 kV is applied between the cathode and anode, which share a common central axis, to ionize Argon (Ar) atoms. The positively charged Ar ions are then accelerated toward the grid or filament located at the throat of the ion source, and subsequently directed towards the target. The ion source generates a highly energetic beam, resulting in films with excellent adhesion and high packing density. The typical pressure during the IBS process is around 10^{-4} Torr, which is lower than the pressure in conventional sputtering processes. This lower pressure is achieved by confining the Ar plasma within the ion source, reducing the chamber pressure and consequently decreasing the impurity rate in the deposited film.

In our case, HfO_2 thin films of varying thickness were fabricated on the cleaned substrates of p^{++}-Si (100) using Hf metal as the target by the IBS method. The films were deposited at 30 % oxygen partial pressure with beam voltage and current of 1000 V and 30 mA, respectively. During deposition, the background pressure and working pressure were maintained at 10^{-6} Torr and 10^{-3} Torr, respectively. The as grown films were subjected to

rapid thermal annealing at 800 °C for 1 hour. HfO_2 thin films of thickness 10, 20 and 30 nm were deposited and denoted as HO10, HO20 and HO30, respectively.

2.3.2 Molecular Beam Epitaxy (MBE)

Molecular beam epitaxy (MBE) is a vacuum deposition technique where precise thermal beams of atoms or molecules react on a crystalline surface to form an epitaxial film. Key features that set MBE apart from other thin film methods include epitaxial growth, a clean ultrahigh vacuum (UHV) environment, in situ characterization during growth, and the absence of highly energetic species. Epitaxy involves depositing a crystalline layer on a crystalline substrate, where the film replicates the substrate's crystal structure. This technique enables the creation of new materials with unexpected properties, such as ferromagnetism at the interface between two antiferromagnetic layers or conductivity between two insulating layers. Utilizing ultrahigh vacuum (UHV) conditions reduces impurities in the deposited films. Achieving high-quality thin films requires precise control of the deposition conditions. A molecular beam is generated inside the chamber either by thermally heating the material in a crucible (effusion cell) or by electron bombardment (e-gun). In an operational MBE system, there are two e-guns, each with four crucibles, and six effusion cells, allowing up to eight different materials to be evaporated simultaneously. Additionally, atomic oxygen is provided by a plasma source. In-situ growth control is facilitated by Reflection High Energy Electron Diffraction (RHEED). A quartz crystal microbalance is also used to monitor the growth rate. The system includes Low Energy Electron Diffraction (LEED) and Auger Electron Spectroscopy (AES) for analyzing surface structure and chemical composition, respectively.

For this work, HfO_2 thin films were fabricated on p^{++}-Si (100) substrates using Hf metal as the target by the MBE technique with a base pressure of 5×10^{-10} mbar. The substrates were cleaned from organic contaminations with ethanol and isopropanol ex situ and vacuum annealed at 1000 °C to remove any impurity from the surface. The films were deposited at 0.2 Å/s for 30 minutes at different substrate temperatures with an oxygen flow at 0.12 standard cubic centimeters per minute (sccm). HfO_2 thin films of thickness ~ 36 nm were deposited by maintaining the temperature of the substrates at 300 and 500 °C, denoted as Film A and Film B, respectively.

2.4 Fabrication of Memory Device

Before deposition, 1×1 cm^2 sized highly doped p-type silicon substrate (p^{++}-Si) was dipped into strong Piranha solution (H_2SO_4 : 30 wt% H_2O_2 = 4 : 1) for 5 minutes to etch the silicon surface for elimination of undesirable native oxide and then washed few times with deionized water. Afterwards, the silicon substrates were sequentially cleaned using acetone and isopropanol for 5 minutes each with the help of ultrasonic bath followed by drying process via passing dry air. The meticulously cleaned p^{++}-Si substrates were then used for deposition of HfO_2 thin films. In order to perform electrical characterization, metal-insulator-metal (MIM) test structures consisting of Al (Ag)/HfO_2/ p^{++}-Si were fabricated with 120 nm thick top electrodes (Al or Ag). Here, p^{++}-Si served as the bottom electrode, whereas aluminum or silver was used for the top electrode material. Using metal shadow mask, the circular Al or Ag top electrode with a diameter of 0.5 mm was deposited on the top of HfO_2/p^{++}-Si using a thermal evaporator under the chamber pressure of ~ 10^{-6} mbar. A schematic representation of the MIM structure is shown in **Figure 2.3**.

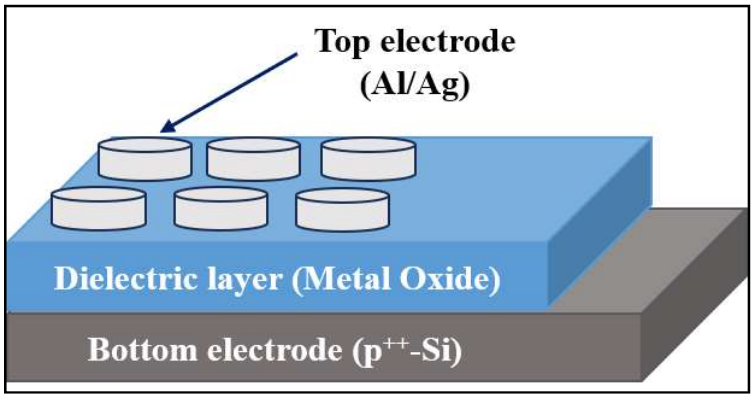

Figure 2.3 *A schematic representation of meta-insulator-metal (MIM) structure.*

2.5 Characterization Techniques

In order to systematically investigate the structure, microstructure, optical, electrochemical and resistive switching behavior of HfO_2 based nanostructures, appropriate characterization techniques have been used in the present work. A brief overview of these characterization techniques is provided below.

2.5.1 X-ray Diffraction (XRD)

X-ray diffraction (XRD) is the most commonly used method for determining the crystal structure of a material. This non-destructive technique is often the first step in characterizing materials to obtain structural properties such as phase formation, crystallite size and lattice strain. XRD works by diffracting an electromagnetic wave with a wavelength of approximately 1 Å off the crystal lattice planes, which are oriented in various directions within the crystal. This diffraction occurs because the X-ray wavelength is of a similar magnitude to the crystal lattice spacing. XRD is essential for identifying different crystalline structures within a material. The technique is based on Bragg's law, which says that incident X-rays are diffracted by a set of equally spaced lattice planes in the crystal, resulting in constructive interference. Constructive

interference happens when the path difference between the diffracted X-rays is an integer multiple of the X-ray wavelength. Bragg's law is expressed as

$$2d\sin\theta = n\lambda \quad \textbf{(2.1)}$$

where d is the interplanar spacing, θ is the Bragg angle, n is the order of diffraction (with n = 1 for XRD) and λ is the X-ray wavelength. A schematic diagram of Bragg's law is presented in **Figure 2.4**.

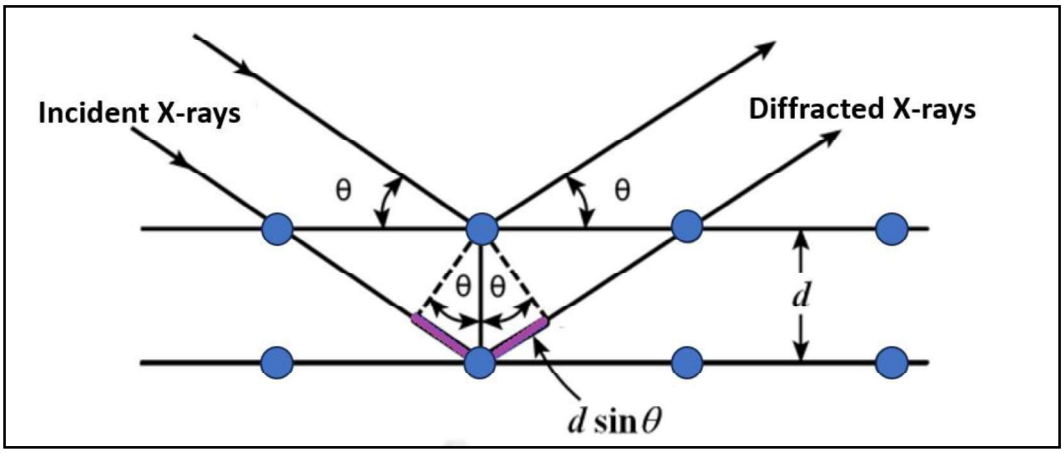

Figure 2.4 *A schematic diagram of incident and diffracted X-rays from equidistance lattice planes in the crystal.*

Due to constructive interference that satisfies Bragg's law, the diffraction pattern shows intense peaks at specific angles of scattering. Generally, crystals with low symmetry, such as monoclinic structures, display numerous diffraction peaks because of their many lattice planes. In contrast, high symmetry structures like cubic and tetragonal crystals exhibit fewer diffraction peaks due to the presence of certain lattice planes. The characteristics and intensities of these diffraction peaks also depend on the size and shape of the crystal particles.

In X-ray diffractometer, an electron beam with the required energy is accelerated towards a copper target to produce X-rays. The collimated characteristic X-rays (Kα) with a wavelength of 1.54 Å are used for material characterization. Most diffractometers operate using the para-focusing or Bragg-Brentano configuration, which is the most common and suitable for various samples. Materials with flat surfaces are easily diffracted, allowing data collection by the detector, which converts the diffracted beam into a count rate. The detector and sample can rotate by angles 2θ and θ, respectively. The resulting plot, showing a series of diffraction peaks as a function of the diffraction angle, is used for crystal structure analysis. XRD data are typically collected in the 2θ range of 10 to 120°.

For our study, XRD data were collected using a Rigaku Miniflex X-ray diffractometer and PANalytical Empyrean powder X-ray diffractometer with Cu Kα (λ = 1.54 Å) operating in Bragg-Brentano geometry. The XRD patterns were indexed using data from the Joint Committee on Powder Diffraction Standards (JCPDS). Structural parameters such as lattice constants and cell volume for the synthesized samples were extracted using Rietveld refinement and Le Bail profile fitting with the FullProf program. This fitting technique matches generated intensities with experimental data to obtain the crystal structure of a specific space group.

2.5.2 Grazing Incidence X-ray Diffraction (GIXRD)

GIXRD operates on the same principle of Bragg's law as in powder XRD. However, when measuring thin films using an XRD instrument designed for powder samples, high-intensity diffraction peaks from the substrates often overshadow the weak signal from the thin film, resulting in a low signal-to-noise ratio and poor structural information about the film. Unlike the Bragg-Brentano geometry, GIXRD employs a low incident angle near the critical angle, with the detector performing a 2θ scan. At this low and constant

incident angle, the X-ray beam does not penetrate deeply into the thin film, enhancing the diffraction signal from the film rather than the substrate.

In our work, for GIXRD, we employed a Rigaku SmartLab equipped with a PhotonMax high-flux 9 kW X-ray source with a rotating Cu anode that produces Cu Kα radiation (λ = 1.54 Å). This system features a high-energy-resolution 2D multidimensional semiconductor detector capable of 0D, 1D, and 2D measurement modes. It includes a high-resolution θ/θ closed-loop goniometer drive system with an in-plane diffraction arm. The integrated Cross-Beam-Optics (CBO) permits automated switching between reflection and transmission optics. GIXRD data were recorded for all the fabricated thin films over a 2θ range of 20 to 80° with a scan rate of 3°/min.

2.5.3 X-ray Reflectivity (XRR)

XRR is a multipurpose and highly sensitive surface characterization method used to measure the thickness of single layer and multilayer thin films, as well as surface density gradients, layer density, surface and interface roughness. For this study, we utilized a Bruker D8 Advance diffractometer with an X-ray source of wavelength 1.54 Å to obtain XRR spectra. Then, to evaluate the thickness, density and roughness of the films, experimental XRR spectra were fitted with appropriate stack models using Parratt32 software.

2.5.4 Raman Spectroscopy

Raman spectroscopy is a non-destructive technique used for chemical analysis, providing detailed information about the chemical structure, phase formation and molecular interactions within a material. Raman spectroscopy can reveal additional information about low-frequency modes and vibrations, offering insights into the crystal lattice or

molecular structure. Raman spectroscopy relies on light scattering, where light interacts with the chemical bonds in a substance. When a high-intensity laser light is scattered by the molecules, most of it retains the same wavelength as the source, known as Rayleigh or elastic scattering. However, some scattered light has different wavelengths due to energy changes that depend on the material's chemical composition or crystallographic structure, known as Raman or inelastic scattering. In Raman scattering, the sample absorbs photons from the laser light and re-emits them at shifted frequencies, providing information about rotational, vibrational, and other low-frequency transitions in molecules or solids.

The experimental setup for Raman spectroscopy includes a Raman spectrometer, a measurement cell and a detector. A laser beam is focused onto a dichroic filter, which reflects the beam at a 90° angle onto the sample. The scattered light of the same wavelength is then refocused onto the dichroic filter, while the Raman scattered light at a different wavelength passes through the filter. Mirrors direct the measured light to a monochromator, which uses a grating to diffract the beam into a narrow range of wavelengths. The detector measures the photocurrent from each wavelength range. For this study, Raman spectra of HfO_2 nanoparticles were recorded between 100 to 800 cm^{-1} using a Raman spectrometer from Jobin Yvon Horiba (HR 800) equipped with an argon laser source with a wavelength of ~ 488 nm.

2.5.5 Fourier Transform Infrared Spectroscopy (FTIR)

FTIR is one of the most common and widely used spectroscopic techniques for characterizing organic and inorganic molecules based on their functional groups. FTIR represents an advancement in converting data from an interference pattern into a

spectrum. FTIR is used to obtain the emission or absorption spectrum of a molecule or atom, which occurs when atoms or molecules transition between energy states.

The most critical component of an FTIR spectrometer is the Michelson interferometer. This interferometer modulates the wavelength of infrared rays emitted from an electrically heated filament source made of rare earth oxides. A grating made of ATR or KBr, which is transparent to infrared radiation, is used to make the radiation monochromatic. A detector measures the intensity of transmitted or reflected radiation for each wavelength (λ). The transmitted portion of the interferogram signals is sent to the detector and analyzed using Fourier transform to produce a single-beam IR spectrum. FTIR spectra are typically displayed as graphs of intensity versus wavenumber (in cm^{-1}), with the intensity plotted as light transmittance or absorbance at specific wavenumbers. In this study, a Thermo Scientific Nicolet Summit FTIR spectrometer was used to record the infrared spectra of HfO_2 samples in the range of 400 to 4000 cm^{-1}.

2.5.6 Transmission Electron Microscopy (TEM)

TEM is mainly utilized to analyze the microstructure of materials, providing essential information about morphology, including the shape and size of particles and their specific size distribution histograms. Various TEM instruments, such as high-resolution TEM (HRTEM), scanning TEM (STEM) and analytical TEM (ATEM), are used for different types of investigations. A standard TEM setup includes an electron gun, a vacuum system, focusing electromagnetic lenses, a high voltage generator and imaging electronic devices. Electromagnetic condenser lenses are used to collimate the electron beam, which has a relatively low wavelength, allowing for excellent resolution below 0.2 nm. A highly focused beam with energy typically exceeding 200 keV is directed at the sample, scattering and partially transmitting towards the objective lens, and imaged on a charge-

coupled device (CCD) camera. In addition to general imaging modes, TEM can generate specific diffraction patterns.

For this study, an FEI Tecnai G^2 20 Twin instrument was used for imaging, selected area electron diffraction (SAED) patterns and high-resolution TEM. Samples were prepared by dispersing 1 milligram HfO_2 powder in 1 ml ethanol The mixture was sonicated for 10 minutes in an ultrasonicator to get homogeneous solution. The sonicated solution was drop casted on the commercial TEM grid (carbon coated copper grid). Thereafter, the grid was dried in vacuum oven to evaporate the ethanol and used for TEM imaging. The size and shape of particles, including their size distribution histograms, were obtained from micrographs and analyzed using ImageJ software. SAED patterns displayed different concentric rings, which were analyzed by evaluating the inverse of their radii and matching them with interplanar spacing (d) calculated from XRD patterns. HRTEM imaging mode unveiled lattice information at the atomic scale, with distinct lattice planes used to estimate the d value corresponding to a specific crystal plane.

2.5.7 Atomic Force Microscopy (AFM)

Electron microscopy is capable of producing two-dimensional images of a sample's surface with ease. In contrast, atomic force microscopy (AFM) can generate a three-dimensional profile of the surface at the nanoscale by measuring the force between a sharp probe tip and the sample surface. The probe tip is attached to a flexible cantilever and lightly contacts the surface, allowing the force between the tip and the surface to be recorded. At very close distances, such as a few angstroms, repulsive Van der Waals forces dominate, indicating the tip and sample are in "contact." When the tip is further from the surface, attractive Van der Waals forces prevail, putting the probe in a non-contact mode. Typically, AFM operates in tapping mode, where the tip oscillates at its

resonance frequency, maintaining a constant oscillation amplitude. Surface roughness, an important material parameter, quantifies the average height of surface features. The root mean square (rms) surface roughness, defined as the average rms. deviation from the average surface height, is commonly used to describe surface roughness.

2.5.8 X-ray Photoelectron Spectroscopy (XPS)

XPS, also known as electron spectroscopy for chemical analysis (ESCA), investigates the elemental composition, oxidation state and valence band structure of a specimen's surface. As a surface-sensitive technique, it primarily provides the relative composition of elements on the surface. XPS is based on the photoelectric effect, where core level electrons are excited by energetic X-ray photons with energy, $h\nu$, resulting in the emission of electrons. The kinetic energy (KE) of these emitted electrons is given by the equation:

$$KE = h\nu - BE - \phi \qquad \textbf{(2.2)}$$

where BE is the binding energy of the electron and ϕ is the work function of the material. Photoelectrons are emitted from the core levels and reach the detector, when the X-ray photon energy exceeds the binding energy and work function of the material. These emitted photoelectrons are identified by their kinetic energy. XPS spectra plot the frequency of emitted electrons as a function of their kinetic energy. The binding energy of different electronic states is calculated relative to the Fermi energy level. For a given photon energy, the kinetic energy distribution of the photoelectrons reflects the energy distribution of electronic states. Photoelectrons can be scattered by nearby electrons, plasmons and phonons, which reduces their kinetic energy and prevents them from passing through the specimen, resulting in an undesirable secondary inelastic background intensity. This scattering is more significant at low kinetic energies due to strong electron-

electron interactions. Although X-rays can penetrate deep into the specimen, only photoelectrons from a few tens of angstroms deep can be detected due to high scattering. To minimize scattering and collisions, the chamber is evacuated to ultra-high vacuum, enhancing the mean free path of the emitted electrons. Monoenergetic soft X-rays are the most suitable energy source for exciting photoelectrons and an electrostatic analyzer is used to analyze them. For this thesis, XPS measurements were performed using Thermo Fisher Scientific X-ray photoelectron spectrometer with Al Kα (1486.6 eV) radiations. The sample preparation chamber was evacuated to ~ 10^{-8} Torr and the analysis chamber maintained at ~ 10^{-9} Torr. An initial survey scan was conducted to collect the full energy range, followed by selective recording of O 1*s*, Hf 4*f*, Pr 3*d* core level spectra for precise elemental analysis and sample composition. All core level spectra were calibrated with respect to the C 1*s* peak centered at 284.6 eV and deconvoluted using XPSPEAK 4.1 software.

2.5.9 Auger Electron Spectroscopy (AES)

Auger electron spectroscopy (AES) is a widely used technique for surface analysis, leveraging the energy of emitted electrons to identify the elements in a sample, much like XPS. The key distinction between the two methods is that XPS uses an X-ray beam to eject an electron, while AES employs an electron beam. In AES, the sample depth analyzed depends on the escape energy of the electrons, unlike XPS, where it is determined by the excitation source. AES is limited to a collection depth of 1-5 nm due to the shallow escape depth of the electrons, enabling the analysis of the first 2-10 atomic layers. Additionally, the typical analysis spot size in AES is approximately 10 nm.

When an inner shell electron of an atom is ejected due to an excitation source (a high-energy electron beam), an outer shell electron must drop to fill the core level. This process

results in either the emission of a secondary X-ray, determined by the energy difference between the orbitals or the ejection of a secondary electron, known as an Auger electron. For example, the ejection of a K shell electron typically leads to an electron from the L shell filling the core level and another L shell electron being ejected as an Auger electron, a process known as the KLL transition. The energy of the Auger electron is measured as kinetic energy in electron volts (eV) and is given by the equation:

$$(KE)_{Auger} = (BE)_K - (BE)_{L1} - (BE)_{L2,3} - \phi \quad \textbf{(2.3)}$$

where $(BE)_K$, $(BE)_{L1}$ and $(BE)_{L2,3}$ are the binding energies of the K, L1 and L2,3 electron orbits of the atom, respectively, and ϕ is the work function. Producing Auger electrons is more efficient for light elements compared to secondary X-rays, making AES particularly sensitive for detecting light elements. However, Auger electrons often have low intensities relative to their background, making their peaks difficult to resolve in a spectrum. Therefore, it is common practice to present the differentiated spectrum to enable identifying and measuring peak positions. We recorded the in-situ Auger electron spectra during the deposition of HfO_2 films through the AES attached to molecular beam epitaxy system.

2.5.10 UV-visible Spectroscopy

A UV-visible spectrophotometer is an optical device used to measure the absorption spectra and determine the band gap of materials. In a double beam spectrophotometer, one beam is directed at the sample, while the other is directed at a standard reference, such as $BaSO_4$ powder. A photomultiplier tube (PMT) is used to record the spectra. A deuterium lamp serves as the UV light source, and a tungsten lamp is used for visible light.

For Pr doped HfO_2 nanoparticles, measurements were conducted in diffuse reflectance mode using an integrating sphere assembly with the Shimadzu 2600 spectrophotometer. The Kubelka-Munk function was used to convert reflectance to absorbance over the range of 200 to 800 nm. Cary 60 UV-visible spectrophotometer was used for the green synthesized HfO_2 nanoparticles. For thin films, Shimadzu 2600 spectrophotometer was used to record the absorption spectra.

2.5.11 Electrochemical Impedance Spectroscopy (EIS)

To measure EIS spectrum, an electrochemical workstation (Gamry's Reference 600 potentiostat) was utilized. We used three-electrode configuration screen printed electrodes (SPEs) from BASi, USA, with 4-mm diameter gold working electrode, gold counter electrode and silver/silver chloride reference electrode. For the preparation of the HfO_2 slurry, we used Polyvinylidene fluoride (PVDF) N-methyl pyrrolidone (NMP) binder (3 wt% PVDF solution in NMP). HfO_2 slurry was prepared by adding 8 mg of HO-4-OPE to 600 µL of DI water in a mortar and pestle. Then, 5 µL of prepared PVDF NMP binder was added to the mortar and pestle and ground the mixture till complete homogeneity. A volume of 400 µL of 200 proof ethanol was added and mixed thoroughly. Afterwards, 10 µL of the above homogeneous mixture was drop-casted on the working electrode and left for 15 min. The coating on the electrode was dried in an oven at 60 °C for 2 h. We targeted six different concentrations of liquid ammonia (50, 100, 200, 300, 400, and 500 ppm) for the EIS measurements. 29 w/w % ammonia solution (Fisher Scientific) was used to prepare the samples for these concentrations with appropriate dilution in deionized water. After completing both ac and dc calibrations of the potentiostat, we used a connector (from PalmSens) to connect the potentiostat with SPEs. We recorded the EIS measurements (at a fixed ac voltage of 10 mV) of HfO_2 sample-

coated SPE at different concentrations of ammonia using a frequency range of 100 mHz to 1 MHz. A schematic diagram of the general set-up for electrochemical measurements with a 3-electrode cell is given in **Figure 2.5 (a)** and the connection set up used by us to measure EIS is shown in the **Figure 2.5 (b).**

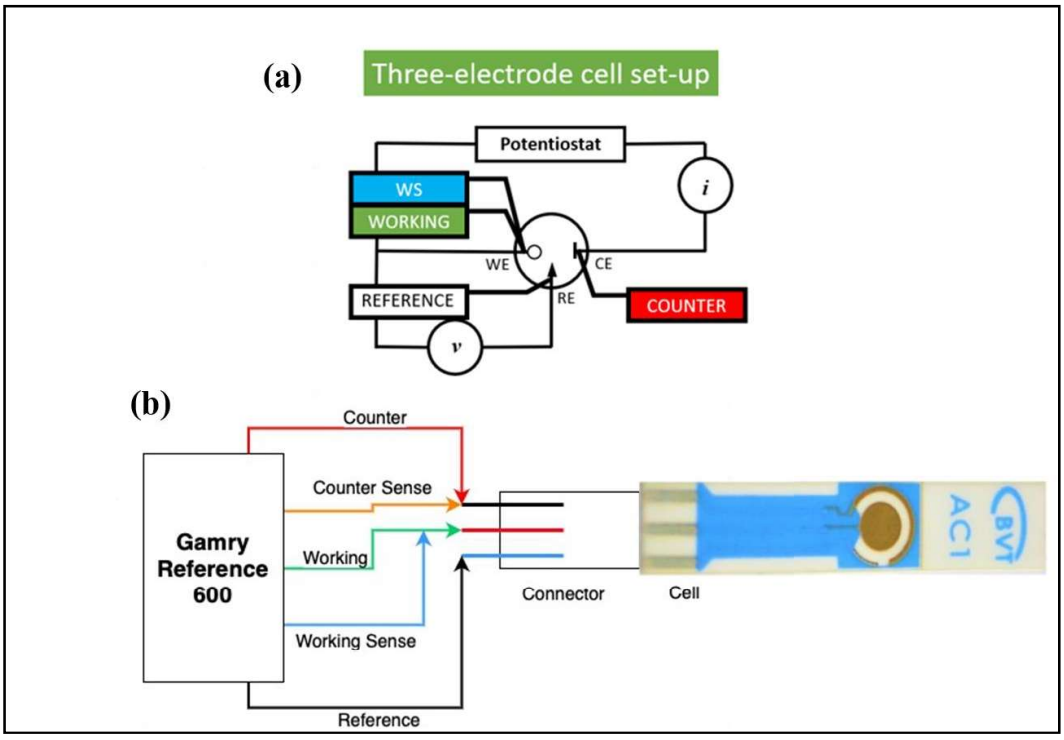

Figure 2.5 *(a) General set-up for 3 electrodes configuration* ***and (b) schematic*** *diagram of our connection of the screen-printed electrode to the Gamry Reference 600 potentiostat (diagram is not to scale).*

2.5.12 Polarization Measurements: *P-V* Hysteresis Loop Tracer

The *P-V* hysteresis loop tracer operates on the basic principle of the Sawyer tower circuit, illustrated in **Figure 2.6**. This circuit features two capacitors in series, one is the test dielectric sample and the other is a linear valued reference capacitor. The reference capacitor's capacitance is set significantly higher than that of the sample to ensure most

of the voltage drops across the sample. The drive voltage in the circuit is nearly equal to the voltage across the sample, while the voltage across the reference capacitor indicates the sample's polarization. These voltages are displayed on the vertical and horizontal plates of an oscilloscope to measure the electric field across the sample. Instead of measuring charges directly, the instantaneous current is measured and then integrated to calculate the charges in an actual *P-V* setup. We measured the *P-V* hysteresis loop using the Precision Premier II ferroelectric loop tracer (Radiant, USA), along with the sample holder unit used in this work.

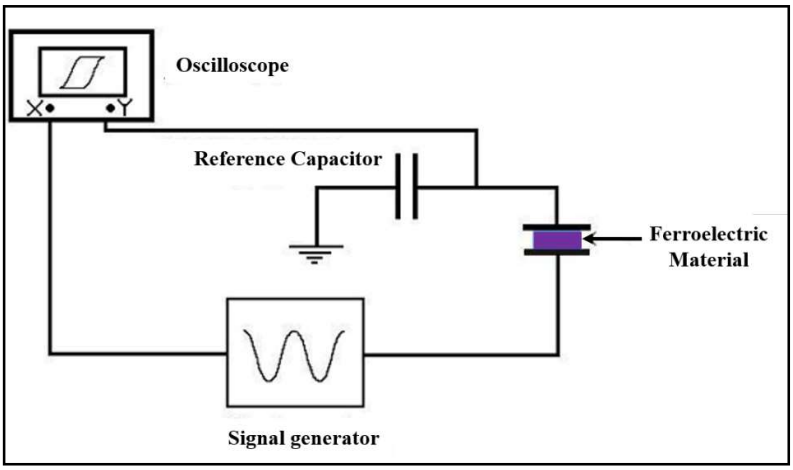

Figure 2.6 *Schematic representation of Sawyer tower circuit for ferroelectric hysteresis measurements.*

2.5.13 Electrical Measurements: *I-V*, Endurance and Retention

The current-voltage (*I-V*) characteristics, endurance and retention measurements of MIM test structures were performed at room temperature under ambient pressure utilizing a semiconductor parameter analyzer. A Keysight parameter analyzer (Model- B1500A) was used for ion beam sputtered HfO_2 films whereas a Keithley (Model- 4200A SCS) parameter analyzer was used for molecular beam epitaxy grown HfO_2 films. *I-V*

characteristics were obtained after sweeping the applied DC bias voltage in a cycle of 0 V→ -3 V→ 0 V→ 3 V→ 0 V for ion beam sputtered films and 0 V → -4 V → 0 V → 1 V → 0 V for molecular beam epitaxy grown films. The electrical contact of MIM structutre was done using a probe micromanipulator. The bias voltage is applied to the top electrode (Al/Ag) while the bottom electrode (p^{++}-Si) is grounded throughout the measurement. To prevent the electrical breakdown of devices, the compliance current (CC) was fixed at 7 mA and 100 µA during all the measurements for ion beam sputtered and molecular beam epitaxy grown thin films, respectilely. The endurance and retention characteristics were examined at a readout voltage of 1 V for the ion beam sputtered HfO_2 film based devices. A schematic diagram of the circuit connection of HfO_2 film based memristor for electrical measurements is shown in **Figure 2.7**.

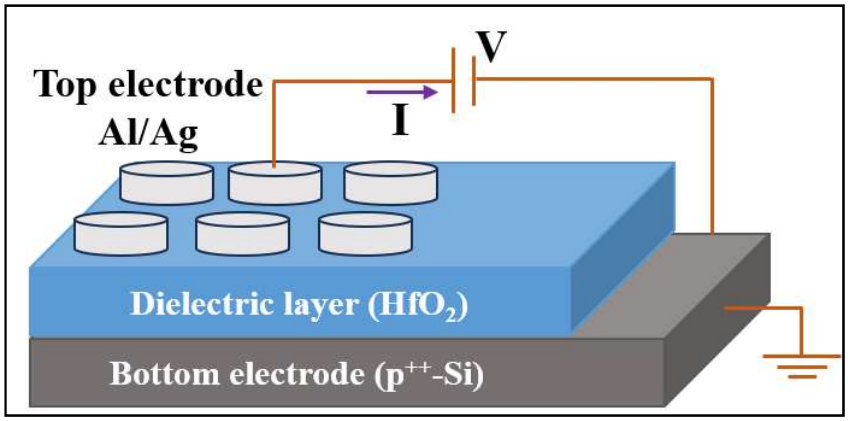

Figure 2.7 *Schematic diagram of the circuit connection of HfO_2 based memristor.*